J. Biochem. **136**, 485–493 (2004)
DOI: 10.1093/jb/mvh148

Bare-Faced Curassow Lysozyme Carrying Amino Acid Substitutions at Subsites E and F Shows a Change in Activity against Chitooligosaccharide Caused by a Local Conformational Change

Tomohiro Araki[1,*], Shinobu Seki[1], Hideki Hirakawa[2], Yuki Chijiiwa[1], Shunsuke Kawamura[1], Satoru Kuhara[2] and Takao Torikata[1]

[1]Department of Bioscience, School of Agriculture, Kyushu Tokai University, Aso, Kumamoto 869-1404; and [2]Faculty of Agriculture, Graduate School of Bioresource and Bioenvironmental Sciences, Genetic Resources Technology, Molecular Gene Techniques, 6-10-1, Hakozaki, Higashi-ku, Fukuoka 812-8581

Received June 4, 2004; accepted July 14, 2004

A new form of avian lysozyme, bare-faced curassow lysozyme (BCL), was purified and chemically sequenced. Of the 26 substitutions relative to chicken lysozyme, three, F34Y, T47S, and R114H, are of substrate-interacting residues in the E and F subsites, which would contribute to the acceptor binding for transglycosylation. T47S is a novel substitution in this lysozyme class. While other lysozymes also have substitutions at positions 114 and 34, they also contain numerous others, including ones in the other substrate binding sites, A–D. Furthermore, T47S lies on the left side, while F34Y and R114H are located on the right side of the E-F subsites. BCL therefore should allow comparison of the independent contributions of these sites to substrate binding and transglycosylation. The activity toward the *N*-acetylglucosamine pentamer revealed that the substitutions at the E-F sites reduced the binding free energies at the E-F sites and the rate constant for transglycosylation without the conformation change of other substrate binding sites on the protein. MD simulation analysis of BCL suggested that the substituted amino acids changed the local conformation of this lysozyme at the E-F sites.

Key words: amino acid sequence, bare-faced curassow, lysozyme; molecular dynamics.

Chicken lysozyme (HEL) is the most studied and best characterized hydrolase; it selectively cleaves the β1-4 glycosidic bonds of *N*-acetylmuramic acid and *N*-acetylglucosamine (GlcNAc) (*1–3*). The tertiary structure of HEL revealed the state of substrate binding as well as conformation of the binding site (*4–6*). Namely, the substrate binding site is composed of six subsites (A-F), and a substrate bound to the subsites is cleaved at subsites D and E through the conventional acid catalytic reaction of Glu35 and Asp52 (*7–13*). This enzyme catalyzes not only hydrolysis of sugar chains but also a transglycosylation reaction that requires an acceptor oligomer instead of a water molecule for hydrolysis (*14*, *15*). Intensive studies on subsites of lysozyme led to the proposal of two distinct binding modes at subsites E and F (*16–18*). The possible mechanism of transglycosylation is: a sugar chain first binds on the left side of the E and F sites and then moves to the right side to be cleaved between sites D and E. The acceptor for transglycosylation occupies the vacant left side and the sugar chain at subsites A–D moves back to the left side after releasing the sugar chain at sites E and F to generate a new chain. However, only a little evidence has been reported because of the difficulties of selective characterization of sites E and F.

While the crystallographic studies of lysozymes on the stable ES complex structure have allowed characterization of sites A to C, it is difficult to obtain information on sites E and F due to rapid hydrolysis of the substrate. Therefore, the structures of sites D, E, and F have been predicted by model building. We previously reported the experimental and simulation evaluation of six subsites using an oligomer substrate, GlcNAc pentamer $(GlcNAc)_5$, followed by computer data-fitting analysis, which enables characterization of sites E and F (*19–22*). Lysozymes carrying the characteristic amino acid mutations at sites E and F will provide the binding free energy of each subsite, and the rate constants for hydrolysis and transglycosylation with this method. However, the change in conformation responsible for the change in activity remains unclear with no direct method for evaluating the conformation change in the presence of a substrate at sites E and F. Molecular dynamics (MD), in contrast, provides a direct picture of movement for a mutant lysozyme with substrate. Thus, the combination of analysis of the experimental time course for an oligomer substrate and MD simulation allows a more detailed characterization of sites E and F.

In the present paper we report the amino acid sequence of bare-faced curassow lysozyme (BCL) carrying characteristic amino acid substitutions at sites E and F determined by a chemical method. We also show the effects of the amino acid substitutions for the GlcNAc oligomer substrate experimentally and by MD simulation.

*To whom correspondence should be addressed. E-mail: taraki@ktmail.ktokai-u.ac.jp

MATERIALS AND METHODS

Purification of Lysozyme—Freshly laid bare-faced curassow (*Crax fasciolata*) eggs were kindly given to us by Ueno Zoological Park, Tokyo, Japan. HEL was purchased from Seikagaku Kogyo Co., Japan. A water extract of egg white was treated by isoelectric precipitation at pH 4.0 and 7.0, and then the clarified solution was put on a CM-Toyopearl column (1.5 × 46 cm) equilibrated with 0.03 M phosphate buffer (pH 7.0). The column was then eluted stepwise with the same buffer containing 0.3 M NaCl. The lysozyme fraction was rechromatographed on the same column with a gradient of 0.1 M to 0.3 M NaCl in the same buffer. Enzyme activity was monitored as lytic activity using lyophilized cell walls of *Micrococcus luteus* as a substrate. Lysozyme solution (10 to 100 μl) was added to the substrate suspension adjusted to OD 1.0 at 540 nm in 3.0 ml of 0.1 M phosphate buffer, pH 7.0, and then the reduction in absorbance at 540 nm was monitored.

Carboxymethylation and Enzymatic Digestion—Reduced and carboxymethylated lysozyme (Cm-lysozyme) was prepared by the method of Crestfield *et al*. (*23*). Cm-lysozyme was digested with trypsin (1:50, w/w, TR-TPCK, Cooper Biomedical Inc., USA) at pH 8.0 and 37°C for 4 h.

Peptide Mapping and Sequence Analysis—The tryptic peptides were separated on a reversed-phase (RP) HPLC column (ODS 120A S5, 4.0 × 250 mm, Yamamura Chemical Co., Japan) in a JASCO 800 series HPLC (Japan Spectroscopic Co., Japan). The peptide elution was performed with a linear gradient elution system of 0.1% trifluoroacetic acid (solvent A) and 60% acetonitrile in solvent A (solvent B). A gradient of 0% to 50% of solvent B was used for 130 min.

Tryptic peptides were hydrolyzed in evacuated sealed tubes at 110°C for 20 h with constant boiling HCl containing 0.05% β-mercaptoethanol. The resulting hydrolysates were analyzed with an amino acid analyzer (Model L-8500, Hitachi Co., Japan). The amino acids of tryptic peptides were sequenced by the DABITC/PITC double coupling manual micro sequencing method (*24*, *25*).

Substrate Binding—Substrate binding was determined by measurement of the fluorescence intensity standardized as to *N*-acetyltryptophane with a Hitachi F-4500 fluorescence photometer. Namely, the GlcNAc trimer $(GlcNAc)_3$ (0.2×10^{-4} M to 2.0×10^{-4} M) was incubated with lysozyme (2.0×10^{-5} M) in 0.01M acetate buffer, pH 5.0, for 5 min at 30°C. The reaction mixture was measured with excitation at 291 nm and emission at 360 nm. The dissociation constant was calculated as the amount of enzyme and substrate complex (reduction of fluorescence intensity of reaction mixture as to that of lysozyme) by Schatchard plotting using the equation $\Delta F = -K_s \times \Delta F/[S] + \Delta F_{Max}$ (ΔF: reduction of fluorescence intensity of reaction mixture as to that of lysozyme; K_s: dissociation constant; [S]: concentration of substrate).

Chemical Modification—Guinea fowl lysozyme (GHL) was modified with diethylpyrocarbonate (DEP). Namely, GHL was incubated with a 100 molar excess of DEP at pH 6 and 25°C for 4 min in 0.1 M phosphate buffer. The resulting reaction mixture was applied to a cation exchange HPLC with a Biofine IEC-CM column (7.5 × 75 mm, Japan Spectro Scopic Co.) in 0.3 M ammonium acetate and eluted with a linear gradient of 0.3 to 0.5 M of the solvent to purify the modified GHL (DEP-GHL) (*26*). Carboxymethylation of GHL was performed with a 100 molar excess of monoiodoacetic acid at pH 6.5 and 40°C for 24 h. The modified GHL (CM-GHL) was purified on a CM Toyopearl column in the same manner as described for the "purification of lysozyme." The obtained CM-GHL was subjected to peptide mapping analysis. The amino acid composition and sequence of the peptide carrying a modified residue detected on the map was analyzed to identify the modified residue at position 114 (His114) (Figs. 1 and 2).

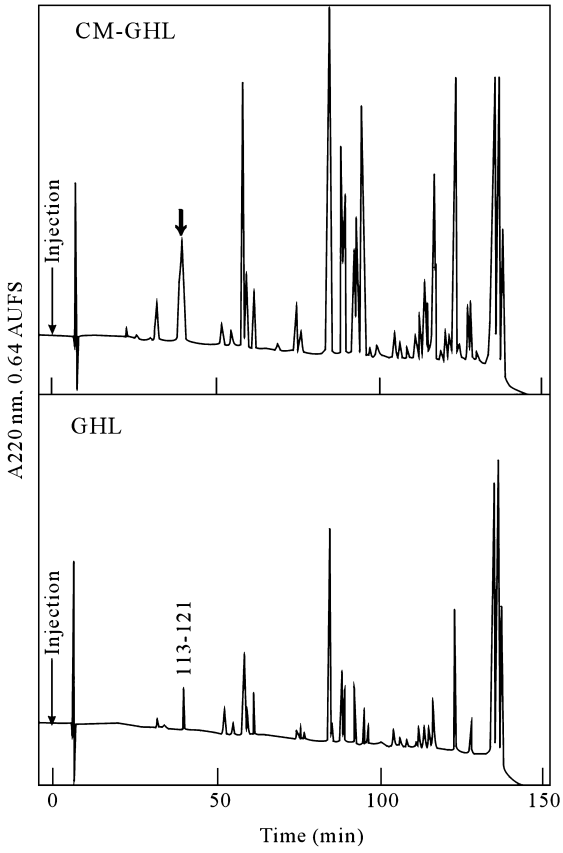

Fig. 1. **Comparison of reversed-phase HPLC peptide maps of monoiodoacetic acid–modified GHL and native GHL.** The peak indicated by an arrow in the modified GHL map was subjected to amino acid composition and amino acid sequence analysis.

Circular Dichroism (CD) Spectra—Circular dichroism (CD) spectra were obtained at 25°C with a JASCO J-820 spectropolarimeter. Proteins were dissolved to a final concentration of 0.15 mg/ml in 0.01 M sodium acetate buffer (pH 5.0). The data were expressed in terms of mean residue ellipticity. The path-length of the cells was 0.1 cm for far-ultraviolet CD spectra (200–250 nm).

Enzyme Action—The measurement of lysozyme activity was performed by the method of Masaki *et al.* (*19*) with a slight modification. Namely, the reaction mixture containing 1×10^{-4} M lysozyme and 1×10^{-3} M $(GlcNAc)_5$ was incubated in 10 mM sodium acetate buffer, pH 5.0, at 50°C. At a given reaction time, 200 μl of the reaction mixture was withdrawn and rapidly chilled in a KOOL KUP

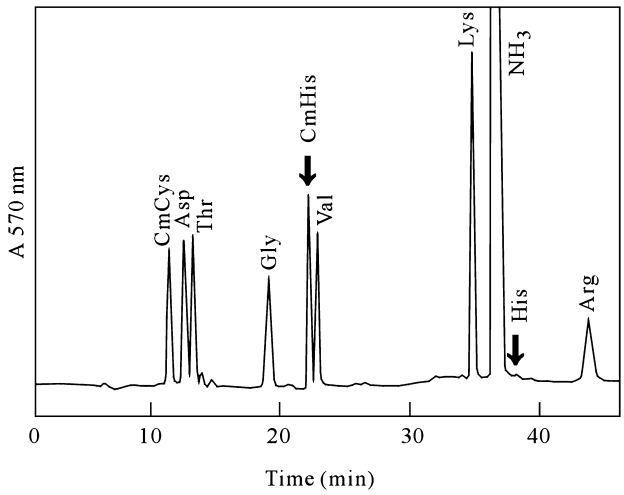

Fig. 2. **Amino acid analysis profile and amino acid sequence of the modified peptide indicated in Fig. 1.** The peak of His indicated by an arrow disappeared and a carboxymethylated His residue was newly detected. The modified His residue is indicated by an asterisk.

(Towa Co., Japan). The reaction mixture was centrifuged with Ultrafree C3LCC (Millipore Co., USA). The filtrate was lyophilized. The dried sample was dissolved in 50 μl of ice-cold water, and then 10 μl of the solution was applied to a TSKgel G-Oligo-PW column (7.8 × 60 mm, Tosoh Co., Japan) in a JASCO 800 series HPLC. Elution was performed with distilled water at room temperature at the flow rate of 0.3 ml/min. Each chitooligosaccharide concentration was calculated from the peak area monitored as ultraviolet absorption at 220 nm, using the standard curve obtained for authentic saccharide solutions.

The rate equation of the lysozyme-catalyzed reaction with the initial substrate $(GlcNAc)_5$ was numerically solved to obtain the calculated time-courses by the method previously reported. In the calculation, the rate equations were solved repeatedly while changing the values of the binding free energies at each of the six binding subsites (A, B, C, D, E, and F), or the rate constants, k_{+1} (cleavage of β-1,4 glycosidic linkage), k_{-1} (regeneration of glycosidic linkage), and k_{+2} (hydration), so that the calculated time-courses fitted those experimentally obtained (Fig. 3).

For data fitting, the time courses were calculated repeatedly by varying the value of the binding free energy change for each of the subsites to obtain a minimum cost function:

$$F = \sum_i \sum_n \left| (\mathrm{GlcNAc})^c_{n,i} - (\mathrm{GlcNAc})^e_{n,i} \right|$$

Here, e and c are the experimental and calculated values, n the size of the chitooligosaccharide, and i the reaction time. A set of values for the reaction parameters giving the minimum value of F in the equation was regarded as the most reliable values for the reaction parameters. For the definition of the cost function, the data for $(GlcNAc)_5$ in the early stage of the reaction were not used, because the chromatographic separation of $(GlcNAc)_5$ and $(GlcNAc)_6$ was not satisfactory in the early stage of the reaction and thus error could not be avoided.

MD Simulations in the ES Complex State—MD simulations were performed using the Discover 95.0 program (Molecular Simulations, San Diego, CA). The AMBER ver.3a force field was used, and the 1–4 nonbond interactions were scaled by a factor of 0.5. The distance-dependent dielectric constant was used for electrostatic interaction. The crystallographic complex structure of HEL and $(GlcNAc)_3$ was obtained from the Protein Data Bank (PDB code: 1hew). Construction of the binding site of the HEL-$(GlcNAc)_6$ complex was started by adding a half-chaired GlcNAc residue to the reducing end of $(GlcNAc)_3$.

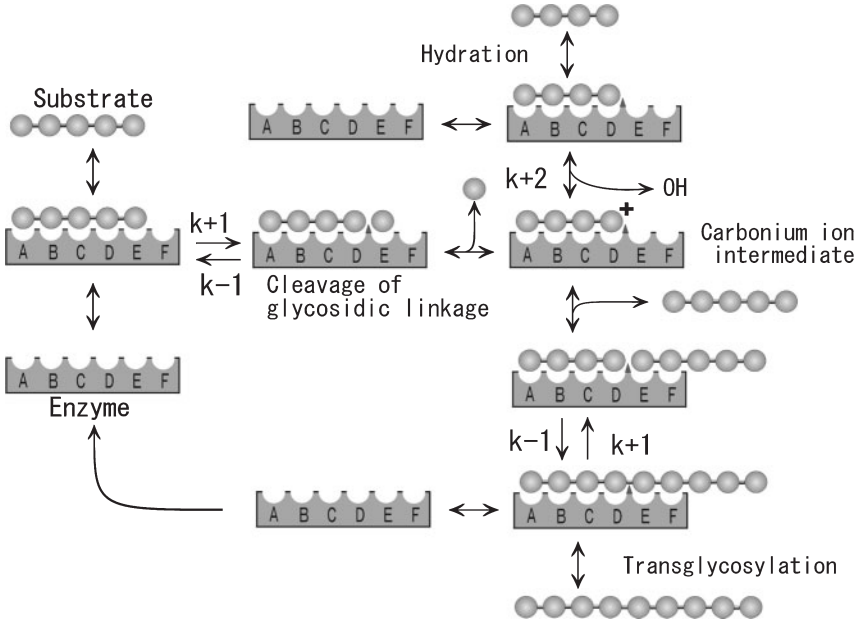

Fig. 3. **Reaction scheme for the lysozyme-catalyzed reaction of the GlcNAc pentamer.** In this scheme, k_{+1}, k_{-1}, and k_{+2} are the rate constants for cleavage of the glycosidic linkage, transglycosylation, and hydration, respectively.

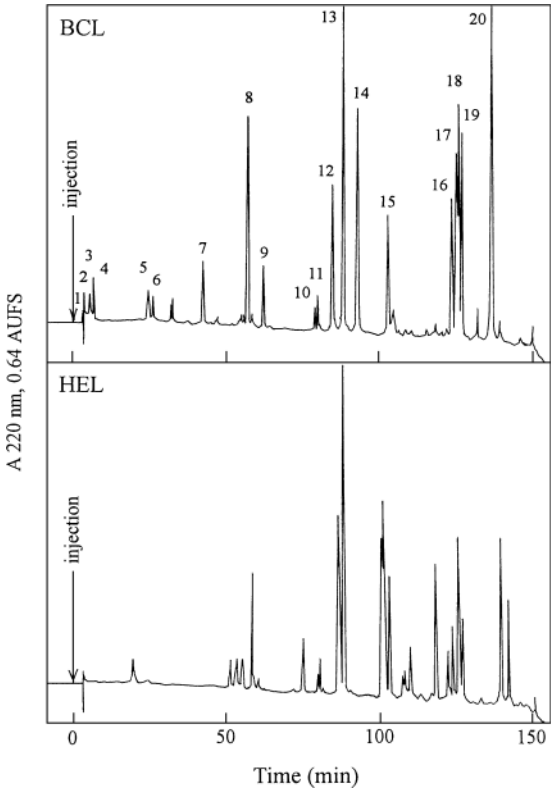

Fig. 4. **Comparison of the reversed-phase HPLC peptide map of BCL with that of HEL.** Peaks numbered in the BCL map were subjected to amino acid composition and amino acid sequence analysis.

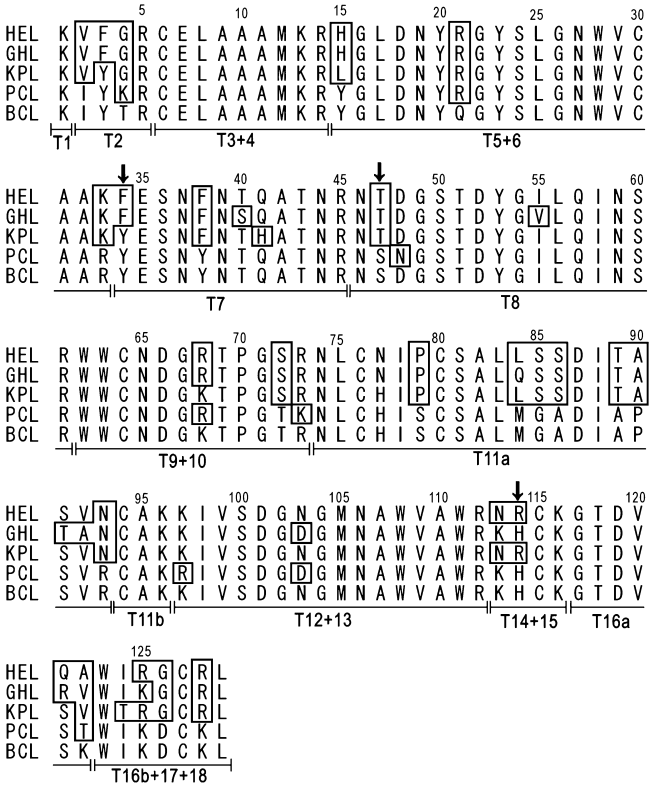

Fig. 5. **Amino acid sequence of BCL, and its comparison with those of HEL, GHL, KPL, and PCL.** The peptides obtained are underlined. Substituted amino acids are boxed. The amino acids indicated by arrows are the substituted amino acids in the substrate binding site.

After $(GlcNAc)_2$ had been bound to the reducing end of the $(GlcNAc)_4$ in the complex, the initial structure of the HEL-$(GlcNAc)_6$ complex was constructed. In this state, the dihedral angle (ϕ and ψ) of $(GlcNAc)_6$ was rotated to avoid steric conflicts. To construct an energetically stable structure, energy minimization was performed until the maximum derivative was less than 0.5 kcal/mol.

The structure of BCL was constructed based on HEL. After 26 amino acid residues of HEL had been replaced using the Insight II package (Molecular Simulations, San Diego, CA), the optimum direction for each side chain was searched for. The conformational structure of the BCL-$(GlcNAc)_6$ complex was constructed as in HEL-$(GlcNAc)_6$ complex.

After the minimization, the complex structure was solvated with a 12.0 Å layer of water molecules and minimized until the maximum derivative was less than 0.5 kcal/mol.

The minimized coordinates were used as a starting point for NVT (constant volume and temperature) molecular dynamics at 300 K to generate possible stable conformations. The system was warmed to 300 K. After a 100 fs equilibration stage, the simulations were continued at 300 K for 200 ps using a 1.0 fs time step. The simulations were carried out using the Verlet velocity algorithm and the structures were stored in a computer every 1.0 ps (*27*).

For MD simulations in the non-complex state, the crystallographic complex structure of HEL was obtained from the Protein Data Bank (PDB code: 1hel). BCL and GHL were constructed by replacing 26 and 10 amino acid residues of HEL, respectively. After the minimization, the structure was solvated with a 12.0 Å layer of water molecules and minimized until the maximum derivative was less than 0.5 kcal/mol. MD simulation was performed for 600 ps.

RESULTS AND DISCUSSION

Purification of BCL—The egg white of bare-faced curassow gave two active peaks on cation exchange chromatography. Multiple expression of chicken-type lysozyme in egg white is a rare phenomenon found only in domestic birds' eggs such as domestic ducks or quails. The specific activities of these isozymes found in bare-faced curassow eggs were considerably different from each other, and the latter isozyme corresponding to the common chicken-type lysozyme (BCL-II) was used as BCL.

Amino Acid Sequence of BCL—For structural analysis, a peptide map of BCL was prepared by RP-HPLC (Fig. 4). As previously reported, we established a rapid structural analysis method involving peptide maps in which a peptide eluted at a different position on comparing two maps contains the substituted amino acid(s) and the peptides eluted in the same positions having identical amino acid compositions, proved to share the identical amino acid sequences in both lysozymes (*28–33*). By comparison of the maps of HEL and BCL, almost all peaks were shown

Table 1. **Amino acid compositions of tryptic peptides of bare-faced curassow lysozyme.**

			∇		∇	∇	∇	∇	∇	∇	
Peptide No.	1	2-1	2-2	3	4	5	6	7	8	9	10
CmCys			0.95(1)	0.83(1)	0.50(1)					0.83(1)	0.90(1)
Asp						1.00(1)			3.18(3)	1.07(1)	
Thr						0.96(1)	2.13(2)	0.99(1)	2.04(2)		
Ser						0.92(1)			0.98(1)		
Glu									2.07(2)		1.01(1)
Pro							0.92(1)				
Gly						0.97(1)	1.16(1)				
Ala				0.78(1)					1.03(1)		3.10(3)
Val						0.89(1)					
Met											0.82(1)
Ile								0.89(1)		0.82(1)	
Leu											0.94(1)
Tyr								0.89(1)	2.08(2)		
Phe											
Lys	1.00(1)		2.00(2)	1.00(1)	1.00(1)	1.00(1)				2.00(2)	1.00(1)
His			0.99(1)		0.56(1)						
Arg		1.00(1)					1.00(1)	1.00(1)	1.00(1)		
Trp										0.53(1)	
Total	1	1	4	3	3	6	5	4	12	6	8
nmol	9.87	1.32	4.43	9.82	5.36	10.04	2.33	4.91	7.09	1.43	3.8
Corresponding peptides of HEL	T1	T4	T14+15	T11b	T14b+15	T16a	T10	T2	T7	T16b+17	T3

		∇	∇	∇	∇		∇			∇
Peptide No.	11	12	13	14	15	16	17	18	19	20
CmCys	0.98(1)	0.90(1)	0.96(1)	0.95(1)			2.00(2)			0.96(1)
Asp		1.92(2)	2.10(2)	1.08(1)	4.33(4)	3.29(3)	2.03(2)	2.89(3)	3.03(3)	2.99(3)
Thr			2.03(2)		1.04(1)					
Ser					2.98(3)	1.11(1)	2.91(3)	0.95(1)	1.06(1)	1.09(1)
Glu	1.00(1)				1.06(1)					1.01(1)
Pro			0.89(1)				1.03(1)			
Gly		1.02(1)	1.99(2)		2.04(2)	2.08(2)	1.04(1)	1.98(2)	1.97(2)	3.15(3)
Ala	2.99(3)					2.06(2)	3.07(3)	2.05(2)	2.26(2)	2.18(2)
Val						1.57(2)	0.88(1)	1.31(2)	1.53(2)	0.94(1)
Met	0.90(1)					0.86(1)	0.92(1)	0.85(1)	0.80(1)	
Ile				0.88(1)	1.95(2)	1.24(1)	2.02(2)	0.43(1)	0.63(1)	
Leu	0.99(1)			0.99(1)	0.95(1)		2.18(2)			2.10(2)
Tyr					1.03(1)					3.21(3)
Phe										
Lys	1.00(1)	1.00(1)	1.00(1)	2.00(2)		1.00(1)				
His							0.94(1)			
Arg	0.88(1)		0.99(1)		1.00(1)	1.01(1)	1.00(1)	1.00(1)	1.00(1)	1.00(1)
Trp		1.61(2)	1.65(2)	0.79(1)		1.66(2)		1.94(2)	1.57(2)	0.68(1)
Total	9	7	12	7	16	16	20	15	15	19
nmol	4.30	3.74	7.62	7.23	8.36	2.08	3.99	1.71	4.18	6.88
Corresponding peptides of HEL	T3+4	T9	T9+10	T16b+17+18	T8	T12+13	T11a	T13	T13	T5+6

to be eluted at the different positions to HEL and this implied that these peptides contained substituted amino acids. To confirm the amino acid substitutions, the amino acid compositions of all peaks numbered in the figure for BCL were analyzed and aligned with the sequence of HEL and that of plain chachalaca lysozyme (PCL), the first lysozyme from the Cracidae (*34*) (Table 1 and Fig. 5). This analysis revealed that every peptide carried amino acid substitutions compared with HEL except for T12+13. T9+10 was eluted at the same position as HEL but had a different amino acid composition, carrying substitutions of Arg68 to Lys, Ser72 to Thr, and Lys73 to Arg, which probably let to the same hydrophobicity of these two peptides. The substituted amino acids, when compared with HEL, were boxed. We found 26 amino acid substitutions in the BCL sequence compared with HEL, and 8 substitutions compared with PCL, which is from a same group of birds, the Cracidae. Of these substitutions, the Phe34 to Tyr, Thr47 to Ser, and Arg114 to His were located at the substrate binding site. Namely, Tyr34 and His114 ware located on the right side of subsites E and F, and Ser47 at the left side of subsites E and F. The substi-

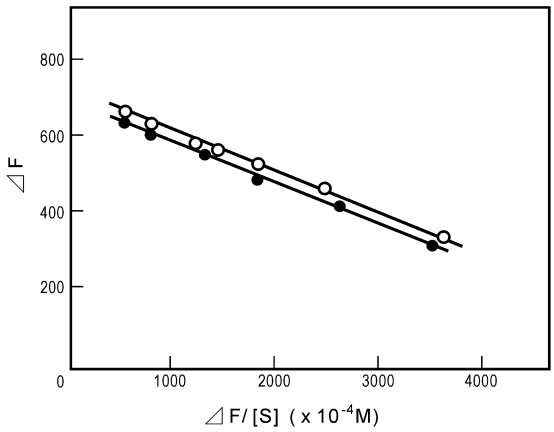

Fig. 6. **Scatchard plotting of binding of BCL and HEL with the GlcNAc trimer.** Solid circles and open circles indicate BCL and HEL, respectively.

tution at position 47 was first found in Galliform lysozymes. It is notable that this lysozyme carried characteristic substitutions only at the E and F sites. In this context, the amino acid sequences of GHL and kalij pheasant (KPL), that carry amino acid substitutions on subsites E and F, are also shown in Fig. 5.

Subsite Structures of A, B, and C—We found that BCL carried amino acid substitutions at subsites E and F, and that this enzyme would be a suitable lysozyme for the study of subsites E and F, which contribute to transglycosylation activity. This enzyme, however, had many amino acid substitutions outside of the substrate binding site in the molecule. To evaluate the conformational change at subsites A–C, we analyzed the fluorescence spectrum caused by the Trp residue with and without the substrate analogue, $(GlcNAc)_3$, and compared it with that of HEL. Chicken type lysozymes have six (A–F) substrate binding sites (subsites), and a substrate bound to subsites is cleaved at subsites D and E through the conventional acid catalytic reaction of Glu35 and Asp52. In lysozyme, the fluorescence intensity derived from Trp residues in subsites A–C (Trp62, Trp63, and Trp108) reflects the microenvironment of the conformation of these sites (*35*, *36*). In this context, the fluorescence signal of lysozyme with a non-productive substrate analogue, $(GlcNAc)_3$, provides the state of substrate binding of the lysozyme and substrate because this trisaccharide preferably binds to subsites A–C in the ratio of 99% without hydrolysis (*4*, *20*).

The obtained Scatchard plot of the binding of $(GlcNAc)_3$ to BCL gave the same slope of the line as in the case of HEL (Fig. 6). The dissociation constant of BCL calculated from the slope of the line was 0.106×10^{-4} M. The calculated dissociation constants, association constants and binding free energies were the same as in the case of HEL, which indicates that BCL binds to the substrate analog in the same manner as HEL. This result indicates that the amino acid substitutions on BCL did not affect the conformational change of subsites A–C compared with HEL.

Furthermore, we analyzed CD spectra in terms of the conformational change caused by the amino acid substitutions. The obtained CD spectra for BCL, HEL and GHL

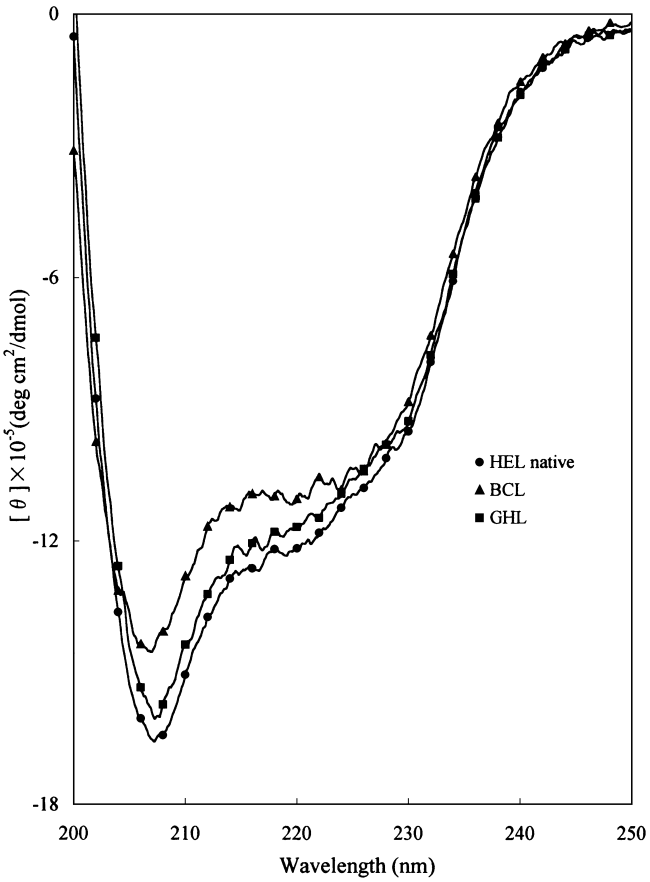

Fig. 7. **Comparison of the circular dichroism spectra of BCL, HEL and GHL.**

were basically similar to each other (Fig. 7). This suggests that the backbone structures of these enzymes are similar, as shown by the binding of $(GlcNAc)_3$. However, BCL exhibited a small difference at 205 to 225 nm, indicating a micro environmental conformational change occurred in BCL when compared with GHL and HEL.

Activity of BCL against GlcNAc Pentamer—For further information on the substrate binding at each subsite, the enzyme was analyzed as to the time-course with $(GlcNAc)_5$, and the results were simulated by computer analysis to obtain the binding free energy and rate constants for each subsite.

As lysozyme catalyzes not only the hydrolysis of sugar chains but also a transglycosylation reaction, the oligosaccharide product shows complicated patterns. However, time course analysis using $(GlcNAc)_5$ enables one to evaluate the effects of amino acids substituted at the subsites by computer simulation analysis (*19*, *20*).

To evaluate the contribution of amino acid substitutions to substrate binding and the lysozyme-catalyzed reaction, the time course of BCL for $(GlcNAc)_5$ was analyzed, and is shown in Fig. 8 with the time courses of HEL, KPL (*29*), GHL, DEP-GHL (*26*), and CM-GHL. Among these lysozymes, KPL carries a substitution at position 34 to Tyr, and GHL carries a substitution at position 114 to His. In the pattern of BCL, the order of the concentrations of the product oligomer at 20 min reaction was 1, 4, 2, 3 instead of 1, 2, 4, 3 for HEL. This

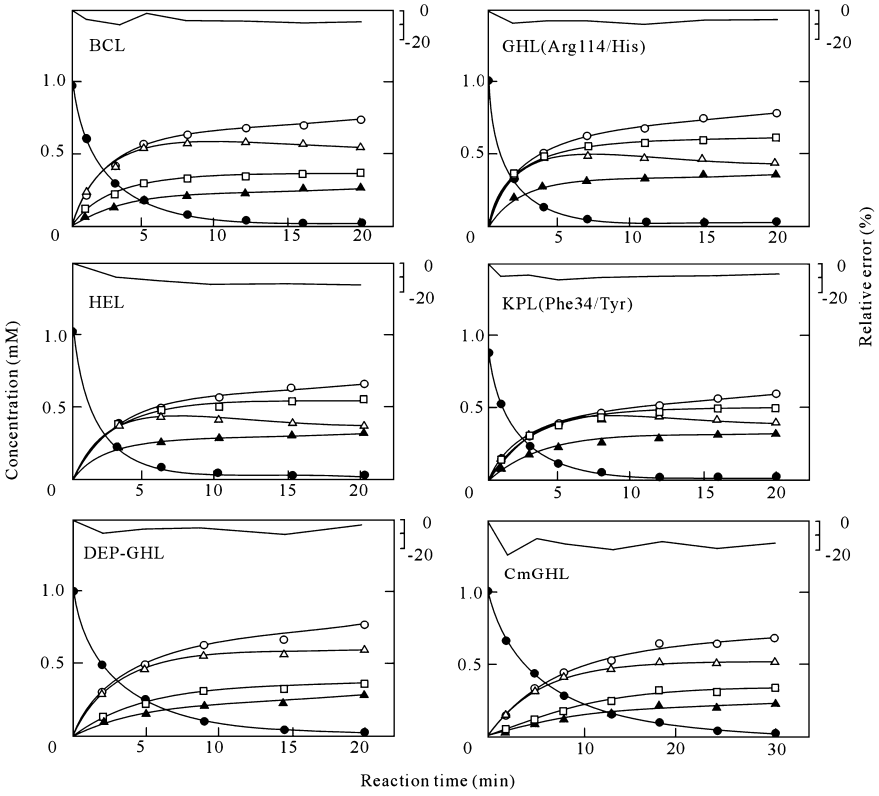

Fig. 8. **Experimental time courses for BCL, HEL, KPL, GHL, DEP-GHL and CM-GHL.** Numerals in the figure indicate the polymerization number of GlcNAc produced through the enzyme action.

pattern was found to be different from those of other lysozymes carrying substitutions at subsites E and F (Fig. 8). This indicates that the characteristic time course pattern of BCL may be caused by the substitution at position 47 on the left side of subsites E and F found as a small difference on comparison of the CD spectra. However, it is noteworthy that DEP-GHL modified at His 114 with diethylpyrocarbonate and CM-GHL modified at the same residue with monoiodoacetic acid showed similar experimental time courses to BCL. This suggests that the local environment of the modified His 114 of GHL changed to be similar to that of BCL.

To confirm this notion, experimental time courses were then simulated by computer analysis. The calculated time courses were constructed by the method of Masaki *et al.* (*19*). The values of binding free energy and rate constant for calculated time courses for these lysozymes are listed in Table 2. The values of binding free energy of BCL for subsites A to D were identical to those of HEL. On the other hand, the values of binding free energy for subsites E and F were observed to be –2.3 kcal/mol at subsite E and –1.3 kcal/mol at subsite F. Furthermore, the rate constant of k_{-1}, the rate of transglycosylation, was also found to be lower than in the case of HEL with a value of 18.5 s^{-1}. This indicates that the substrate binding for BCL is different from for HEL at subsites E and F, and the binding ability of the acceptor for transglycosylation is reduced compared with in the case of HEL. KPL and GHL carrying the substituted amino acids at subsites E and F showed different values compared to BCL. This might be a combined effect of amino acid substitutions at subsites E and F on BCL. However, DEP-GHL showed identical values to BCL. CM-GHL also showed identical values of binding free energy. The lower k_{-1} value found for CM-GHL may due to the size of the introduced group. This result suggests that the microenvironment of His 114 of BCL is changed compared with that of HEL to cause a reduction in the rate constant of transglycosylation, such as modification of His 114 on GHL.

In the lysozyme action, a sugar chain first binds on the left side of subsites E and F, and then moves to the right side to be cleaved between subsites D and E. Then the acceptor for transglycosylation occupies the vacant left side and the sugar chain at subsites A–D moves back to

Table 2. **Estimated values of binding free energies for BCL, HEL, KPL, GHL and CM-GHL.**

	Binding free energy (kcal/mol)						Rate constant (s^{-1})		
	A	B	C	D	E	F	k_{+1}	k_{-1}	k_{+2}
BCL	–2.0	–3.0	–5.0	+4.5	–2.3	–1.3	0.93	18.5	0.3
HEL	–2.0	–3.0	–5.0	+4.5	–2.5	–1.5	0.93	40.0	0.3
KPL	–2.0	–3.0	–5.0	+4.5	–2.4	–1.4	0.93	40.0	0.3
GHL	–2.0	–3.0	–5.0	+4.5	–2.5	–1.5	0.93	35.0	0.3
CM-GHL	–2.0	–3.0	–5.0	+4.5	–2.3	–1.3	0.93	20.0	0.3
DEP-GHL	–2.0	–3.0	–5.0	+4.5	–2.3	–1.3	0.93	18.5	0.3

Table 3. **Distances between a substrate and Glu 35 and Arg (His) 114 determined by molecular dynamics (MD) symulations.**

		No. of detectd pair (4.0 Å ≤)	Distance (Å)	Standard deviation (Å)
Glu35-NAG4	Initial	15/26	9.25/7.50	2.84/2.14
	MD	10/14	9.86/7.97	2.70/2.11
Arg114 (His114)-NAG6	Initial	41/24	7.14/7.41	1.98/2.12
	MD	12/0	8.09/9.54	2.07/1.82

[a]HEL/BCL.

the left side after releasing the sugar chain at subsites E and F to generate a new chain. High transglycosylation performance may require enough space for the binding of the acceptor at subsites E and F. To clarify the location and movement of each amino acid, tertiary structure comparison is invaluable.

MD simulations of BCL—To elucidate the conformational change at subsites E and F, we constructed the tertiary structure of BCL by molecular modeling. The conformational structure in the non-complex state of BCL was compared with those of HEL and GHL. Although the overall structure of BCL was similar to those of HEL and GHL, the structure on the left side of BCL was different from that of HEL and GHL. At subsites E and F, the location of the amino acid at position 47 of BCL (Ser47) was shifted from that of HEL and GHL, accompanied by the movement of the main chain (Fig. 9). The conformation of the side chain at position 114 of BCL was also different from that of HEL and GHL. On the other hand, the orientation of the side chain of amino acid residue at position 34 was slightly changed from that of HEL and GHL (Fig. 9). His 114 of BCL shifted to the upper left in spite of no substitution in GHL in this region (Fig. 9). BCL showed the same activity pattern as DEP-GHL and CM-GHL. Therefore, the different location of the His residue found between native GHL and BCL at position 114 may contribute to the substrate-binding at subsites E and F of BCL, and coincide with the result for modified GHL. To evaluate the movement of His 114 of BCL in the complex state, the distances between $(GlcNAc)_6$ located by MD simulation and Arg 114 of HEL and His 114 of BCL were calculated for 50 structures from 101ps to 150ps (Table 3). An atom pair for His 114 of BCL within 4.0 Å distance from NAG6 (6th GlcNAc from non-reducing end) was not found. The average value of the distance between His 114 and NAG6 of BCL was shifted (1.5 Å) far from that of HEL. The change in the value of binding free energy for subsites E and F, and the rate constant of transglycosylation found for BCL may be ascribable to this movement of His 114 reducing the accessibility of substrate. An other possibility for the difference is the substitution at position 47 of Ser on the left side, which may cause the change of acceptor binding at the left side of subsites E and F.

In conclusion, we experimentally and computationally found that conformational changes at amino acid residues at positions 34, 47 and 114 based on amino acid substitutions in subsites E and F on BCL affected the enzymatic activity and binding affinity of substrates. This may be confirmed by further work on the identification of these amino acids by site-directed mutagenesis.

We would like to thank Dr. Hidemasa Hori of Ueno Zoological Park for supplying the eggs. Data deposition: The sequence reported in this paper has been deposited in the PIR database (accession No. JE0185). This work was partially supported by a Grant-in-Aid for Scientific Research on Priority Areas from the Ministry of Education, Science, Sports and Culture of Japan, and by the Research for the Future Program of the Japan Society for the Promotion of Science. Computation time was provided by the Supercomputer Laboratory, Institute for Chemical Research, Kyoto University.

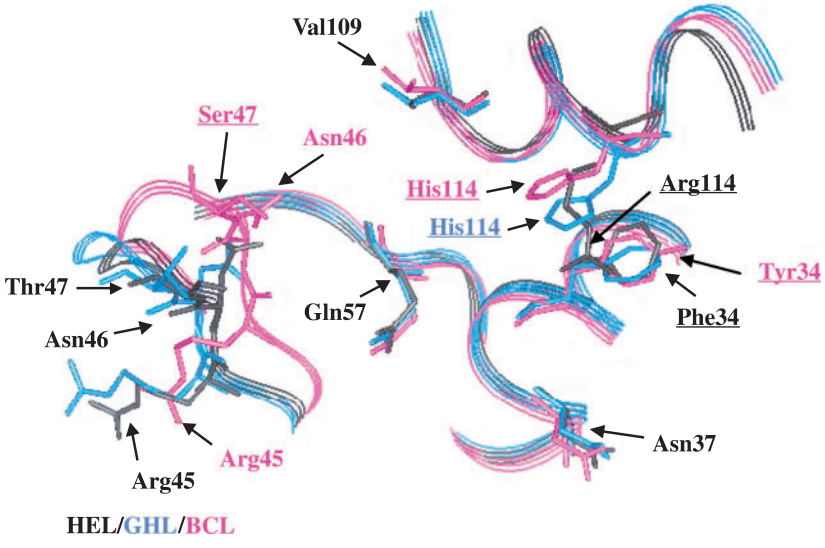

Fig. 9. **Comparison the structures of the E–F sites of BCL, HEL and GHL in the non-complex state.** These structures were averaged from 300 to 600 ps on MD simulation. The main chain structures of HEL, GHL and BCL were shown as ribbon models. The mutated amino acids in BCL located at the different positions from those in HEL or GHL are underlined.

REFERENCES

1. Canfield, R.E. (1963) The amino acid sequence of egg white lysozyme. *J. Biol. Chem.* **238**, 2698–2707
2. Jollès, J., Jauregui-Adell, J., Bernier, I., and Jollès, P. (1963) La structure chimique du lysozyme de blanc d'oeuf de poule: etude detaillee. *Biochim. Biophys. Acta* **78**, 668–689
3. Jung, A., Sippel, A.E., Grez, M., and Schutz, G. (1980) Exons encode functional and structural units of chicken lysozyme. *Proc. Natl Acad. Sci. USA* **77**, 5759–5763
4. Kelly, J.A., Sielecki, A.R., Sykes, B.D., James, M.N.G., and Phillips, D.C. (1979) X-ray crystallography of the binding of the bacterial cell wall trisaccharide NAM-NAG-NAM to lysozyme. *Nature* **282**, 875–878
5. Pincus, M.R. and Scheraga, H.A. (1981) Prediction of the three-dimensional structures of complexes of lysozyme with cell wall substrates. *Biochemistry* **20**, 3960–3965
6. Pincus, M.R., Zimmerman, S.S., and Scheraga, H.A. (1977) Structures of enzyme-substrate complexes of lysozyme. *Proc. Natl Acad. Sci. USA* **74**, 2629–2633
7. Kuroki, R., Ito, Y., Kato, Y., and Imoto, T. (1997) A covalent enzyme-substrate adduct in a mutant hen egg white lysozyme (D52E). *J. Biol. Chem.* **272**, 19976–19981
8. Hashimoto, Y., Yamada, K., Motoshima, H., Omura, T., Yamada, H., Yasukochi, T., Miki, T., Ueda, T., and Imoto, T. (1996) A mutation study of catalytic residue Asp 52 in hen egg lysozyme. *J. Biochem.* **119**, 145–150
9. Parsons, S.M., Jao, L., Dahlquist, F.W., Borders Jr, C.L., Racs, J., Groff, T., and Raftery, M.A. (1969) The nature of amino acid side chains which are critical for the activity of lysozyme. *Biochemistry* **8**, 700–712
10. Parsons, S.M. and Raftery, M.A. (1969) The identification of aspartic acid residue 52 as being critical to lysozyme activity. *Biochemistry* **8**, 4199–4205
11. Yamada, H., Imoto, T., and Noshita, G. (1982) Modification of catalytic groups in lysozyme with ethylenimine. *Biochemistry* **21**, 2187–2192
12. Kuroki, R., Yamada, H., Moriyama, T., and Imoto, T. (1986) Chemical mutations of the catalytic carboxyl groups in lysozyme to the corresponding amides. *J. Biol. Chem.* **261**, 13571–13574
13. Hornbeck, P.V. and Wilson, A.C. (1984) Local effects of amino acid substitutions on the active site region of lysozyme: a comparison of physical and immunological results. *Biochemistry* **23**, 998–1002
14. Pollock, J.J. and Sharon, N. (1970) Studies on the acceptor specificity of the lysozyme-catalyzed transglycosylation reaction. *Biochemistry* **9**, 3913–3925
15. Fukamizo, T., Goto, S., Torikata, T., and Araki, T. (1989) Enhancement of transglycosylation activity of lysozyme by chemical modification. *Agric. Biol. Chem.* **53**, 2641–2651
16. Smith-Gill, S.J., Rupley, J.A., Pincus, M.R., Carty, R.P., and Scheraga, H.A. (1984) Experimental identification of a theoretically predicted "left-sided" binding mode for (GlcNAc)6 in the active site of lysozyme. *Biochemistry* **23**, 993–997
17. Inoue, M., Yamada, H., Yasukochi, T., Miki, T., Horiuchi, T., and Imoto, T. (1992) Left-sided substrate binding of lysozyme: evidence for the involvement of asparagine-46 in the initial binding of substrate to chicken lysozyme. *Biochemistry* **31**, 10322–10330
18. Araki, T., Yamamoto, T., and Torikata, T. (1998) Reptile lysozyme: the complete amino acid sequence of soft-shelled turtle lysozyme and its activity. *Biosci. Biotechnol. Biochem.* **62**, 316–324
19. Masaki, A., Fukamizo, T., Otakara, A., Torikata, T., Hayashi, K., and Imoto, T. (1981) Estimation of rate constants in lysozyme-catalyzed reaction of chitooligosaccharides. *J. Biochem.* **90**, 1167–1175
20. Kuhara, S., Ezaki, E., Fukamizo, T., and Hayashi, K. (1982) Estimation of the free energy change of substrate binding lysozyme-catalyzed reactions. *J. Biochem.* **92**, 121–127
21. Fukamizo, T., Ikeda, Y., Ohkawa, T., and Goto, S. (1992) 1H-NMR study on the chitotrisaccharide binding to hen egg white lysozyme. *Eur. J. Biochem.* **210**, 351–357
22. Fukamizo, T., Minematsu, T., Yanase, Y., Hayashi, K., and Goto, S. (1986) Substrate size dependence of lysozyme-catalyzed reaction. *Arch. Biochem. Biophys.* **250**, 312–321
23. Crestfield, A.M., Moore, S., and Stein, W.H. (1963) The preparation and enzymatic hydrolysis of reduced and S-carboxymethylated proteins. *J. Biol. Chem.* **238**, 622–627
24. Chang, J.Y., Brauer, D., and Wittmann-Liebold, B. (1978) Micro-sequence analysis of peptides and proteins using 4-NN-dimethyl-aminoazobenzene 4′-isothiocyanate/phenylisothiocyanate double coupling method. *FEBS Lett.* **93**, 205–214
25. Yang, C.Y. (1979) Die trennung der 4-[4-(dimethylamino) phenylazo] phenylthiohydantoin-derivate des leucins und isoleucins uber polyamid-dunnschichtplatten im picomol-bereich. *Hoppe-Seyler's Z. Physiol. Chem.* **360**, 1673–1675
26. Kuramoto, M., Fukamizo, T., Araki, T., and Torikata, T. (1997) Study on subsites E and F of lysozyme. *Proc. Sch. Agric. Kyushu Tokai Univ.* **16**, 39–46
27. Swope, W.C., Andersen, H.C., Berens, P.H., and Wilson, K.R. (1982) A computer simulation method for the calculation of equilibrium constants for the formation of physical clusters of molecules: application to small water clusters. *J. Chem. Phys.* **76**, 637–649
28. Araki, T., Kuramoto, M., and Torikata, T. (1990) The amino acid sequence of lady Amherst's pheasant (Chrysolophus amherstiae) and golden pheasant (*Chrysolophus pictus*) egg-white lysozymes. *Agric. Biol. Chem.* **54**, 2299–2308
29. Araki, T., Kudo, K., Kuramoto, M., and Torikata, T. (1991) The amino acid sequence of lysozyme from kalij pheasant egg-white. *Agric. Biol. Chem.* **55**, 1701–1706
30. Araki, T., Kuramoto, M., and Torikata, T. (1991) The amino acid sequence of reeves' pheasant lysozyme. *Agric. Biol. Chem.* **55**, 1707–1713
31. Araki, T., Kudo, K., Kuramoto, M., and Torikata, T. (1989) The amino acid sequence of Indian peafowl (*Pavo cristatus*) lysozyme and its comparison with lysozymes from phasianoid birds. *Agric. Biol. Chem.* **53**, 2955–2962
32. Araki, T., Kuramoto, M., and Torikata, T. (1994) The amino acid sequence of copper pheasant lysozyme. *Biosci. Biotechnol. Biochem.* **58**, 794–795
33. Araki, T., Matsumoto, T., and Torikata, T. (1998) The amino acid sequence of monal pheasant lysozyme and its activity. *Biosci. Biotechnol. Biochem.* **62**, 1988–1994
34. Jollès, J., Schoentgen, F., Jollès, P., Prager, E.M., and Wilson, A.C. (1976) Amino acid sequence and immunological properties of chalchalaca egg white lysozyme. *J. Mol. Evol.* **8**, 59–78
35. Maenaka, K., Kawai, G., Watanabe, K., Sunada, F., and Kumagai, I. (1994) Functional and structural role of a tryptophan generally observed in protein-carbohydrate interaction. TRP-62 of hen egg white lysozyme. *J. Biol. Chem.* **269**, 7070–7075
36. Nishimoto, E., Yamashita, S., Yamasaki, N., and Imoto, T. (1999) Resolution and characterization of tryptophyl fluorescence of hen egg-white lysozyme by quenching- and time-resolved spectroscopy. *Biosci. Biotechnol. Biochem.* **63**, 329–336